Uniform sensing layer of immiscible enzyme-mediator compounds developed via a spray aerosol mixing technique towards low cost minimally invasive microneedle continuous glucose monitoring devices

Siamak Samavat[a], Jonathan Lloyd[a], Laura O'Dea[a] Wei Zhang[a], Emily Preedy[a], Stephen Luzio[b] and Kar Seng Teng[a]*

[a]College of Engineering, Swansea University, Bay Campus, Fabian Way, Swansea SA1 8EN, UK.

[b]Institute of Life Sciences, Swansea University, Singleton Campus, Singleton Park, Swansea, SA2 8PP, UK.

*Corresponding author: k.s.teng@swansea.ac.uk

Abstract

In this study, a uniformly mixed sensing layer of typically immiscible compounds, such as tetrathiafulvalene (TTF) mediator and glucose oxidase (GOx) enzyme, was developed using a simultaneous spray deposition technique ideal for mass production of glucose sensors at low cost while exhibiting enhanced amperometric response. For comparison, the sensors were fabricated via three different methods: conventional drop-cast of TTF and GOx compounds in subsequent layers (DL), spray deposition of the compounds in subsequent layers (SL), and spray mixing of the compounds as one uniform layer (SM). Uniformity of the sensing layers was investigated via Scanning Electron Microscopy (SEM) and Energy Dispersive X-Ray Spectroscopy (EDX) techniques demonstrating an even distribution of the TTF and GOx throughout the sensing layer for the SM sensors. The amperometric studies showed a significantly larger maximum current response, I_{max} and sensitivity for the SM sensors as compared to the SL and DL sensors. The significantly better performance of the SM sensors correlated well with the even distribution of TTF and GOx throughout the sensing layer, resulting in enhanced electron transfer and redox reaction between GOx and TTF. The SM

spray technique was then applied to deposit a uniformly mixed sensing layer on to 3D microneedle arrays to provide minimally invasive continuous glucose monitoring (CGM). In-vivo studies showed amperometric response from the microneedle CGM device was compatible to changes in blood glucose levels measured via the standard finger prick tests. Importantly, the deposition technique is suitable for mass production of the microneedle CGM at very low cost.

Key Words

Diabetes; sensor; continuous glucose monitoring; microneedles; spray coating; glucose oxidase.

1 Introduction

Diabetes is a long-term chronic illness which requires good management to delay or prevent further health complications. It has been predicted that diabetes will be the 7th leading cause of death by 2030 (Mathers and Loncar 2006) leading to an increasing demand in glucose monitoring devices for diabetes (Chen et al. 2013). Enzymatic electrochemical glucose sensors are well-established due to low cost, good selectivity and stability, particularly the second generation glucose sensors are favourable (Chaubey and Malhotra 2002; Chen et al. 2013; Wilson and Turner 1992).

Kausaite-Minkstimiene et al. reported TTF mediated glucose sensors exhibited excellent performance as compared to sensors with other common mediators (Kausaite-Minkstimiene et al. 2014). TTF as a water insoluble mediator provides a stable immobilization in contact with aqueous media, hence making it suitable for use in implantable devices (Chen et al. 2013; Hale et al. 1989; Kausaite-Minkstimiene et al. 2014). The immobilization of the mediator both near the enzyme's redox center and the electrode's surface is important for electron transfer between the mediator, the enzyme, and the electrode (Chen et al. 2013; Haiying and Jiaqi 1995). This can be improved by good mixing of the mediator and enzyme throughout the sensing layer.

Drop casting is the most commonly used method for the deposition of sensing elements to produce low cost biosensor (Chaubey and Malhotra 2002; Chen et al. 2013). However, this method often lead to 'coffee ring' effect and non-uniform distribution of the drop-cast

compounds on the surface (Liu and Yu 2011). Previously, Kausaite-Minkstimiene et al reported insignificant difference in sensor performances for mixed and layer-by-layer drop casting of TTF and GOx (Kausaite-Minkstimiene et al. 2014). TTF and GOx are almost immiscible due to their poor solubility in aqueous and organic solvents respectively (Nielsen et al. 2000; Singer 1963; Zaks and Klibanov 1985), therefore uniform mixture of these two compounds could not be achieved via the conventional drop-cast method.

To address this challenge, mixing of TTF and GOx compounds was performed using a spray coating deposition technique developed in this work. In this study, the TTF and GOx compounds were deposited successively via the conventional drop-cast method (DL) as well as spray layer-by-layer method (SL), and compared with simultaneous spray mixing method (SM). The SM technique allowed the TTF and GOx to mix as aerosol particles to produce a uniformly mixed sensing layer. The planar uniformity as well as cross-sectional distribution of the TTF and GOx compounds was investigated via SEM imaging and EDX analysis. Furthermore, the amperometric response of the sensors were studied and evaluated. The uniform mixing of TTF and GOx is expected to maximize the redox active interface between the two materials enhancing the amperometric response to glucose. In this study, the novel use of spray coating technique was demonstrated to fabricate a uniform sensing layer consisting of immiscible compounds in order to produce sensitive, low-cost, and mass producible glucose sensors. The SM technique, which produced glucose sensor with the best biosensing performance, was then applied to deposit the sensing layer onto three dimensional (3D) microneedle arrays for minimally invasive continuous glucose monitoring (CGM). Such SM technique can also be used to fabricate a wide range of biosensors at very low-cost.

2 Materials and Methods

2.1 Materials

Aspergillus Niger GOx (270 U/mg) was purchased from BBI solutions Ltd, UK. TTF, 0.01 M sterile phosphate buffer solution (PBS used as the supporting electrolyte for the electrochemical studies), D glucose anhydrous, paraffin wax, Tetrahydrofuran (THF), Methyl Ethyl Ketone (MEK) and extra pure deionised water were purchased from Fisher Scientific, UK. Glutaraldehyde (25%), diacetone alcohol and polyurethane (PU) were purchased from Sigma Aldrich, UK. Graphene based carbon ink (HDPlas® IGSC02002) was purchased from

Haydale, UK. SU8-2075 was purchased from A-Gas Electronic Materials. 126-49 - Silicone Medical Electrode Ag/AgCl Ink was purchased from Creative Materials Ltd. Details on the solutions preparation are provided in Supporting Information, section 1.

2.2 Apparatus

Iwata Eclipse CS spray guns were purchased from Airbrushes UK. All the reagents were of analytical grade and used without further purification. A rotating stage was designed and fixed at a rotation speed of 12 rpm to ensure uniform coating of the 3D microneedle arrays. Uniformity of the TTF and GOx in the fabricated sensors was studied using SEM and EDX techniques. SEM imaging and EDX analysis were performed using a Hitachi S-4800 SEM equipped with an Oxford instruments EDX detector for topographical and elemental analysis respectively. UV–VIS spectroscopy (UV-VIS) was performed using a Hitachi U2900 to determine the quantity of the spray deposited compounds (see Supporting Information, section 2).

Amperometric measurements in beaker were performed using an Ivium CompactStat from Alvatek. The in-vivo testing of the microneedles CGM was performed using an EMSTAT3 Blue from PalmSense Ltd. The device was limited to a maximum potential of 5V to avoid accidental exposure of skin to high electrical potential.

2.3 Sensor Fabrication

The glucose sensors were fabricated by first spray coating a conductive carbon layer onto heat resistive flexible polyimide substrate and subsequently depositing the sensing compounds. To produce the conductive layer of the working electrodes, 0.15 mm thick polyimide sheets were cut into 1.4 x 0.7 cm rectangular shapes. 5 g of the carbon paste was mixed in 20 g of diacetone alcohol to achieve a 4:1 solvent to carbon paste ratio, which was then spray deposited to form the conductive layer for the working electrodes. After spray deposition, carbon electrodes were annealed on a hot plate at 250 °C for 10 min. Resistance of the conductive layer was measured using a standard multimeter and found to be approximately 200 Ω across 1.4 cm along the electrodes. The conductive carbon electrodes were subsequently coated with TTF and GOx sensing compounds via three different

fabrication methods (Scheme 1). Details on the different fabrication methods are provided in Supporting Information, section 3.

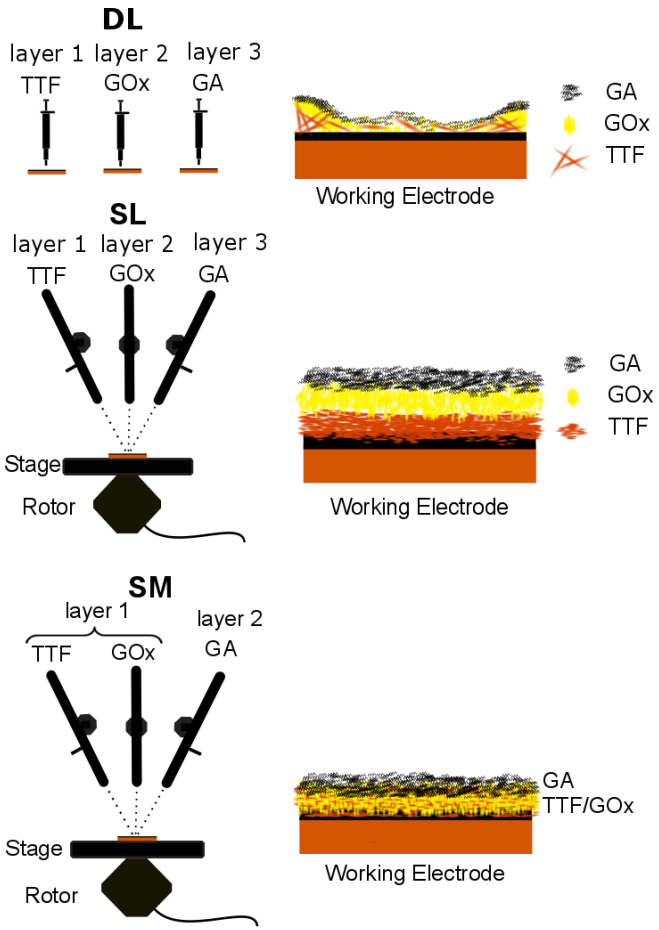

Scheme 1: The schematic diagrams of the drop-cast in layers (DL), sprayed in layers (SL), and spray mixing (SM) of the sensing compounds.

2.4 Electrochemical cell set-up

Amperometric measurements were performed in an electrochemical cell consisting of a fabricated working electrode (area 0.09 cm^2), an Ag/AgCl reference electrode and a gold wire counter electrode at 0.3 V, which is the established oxidation potential for TTF mediator (Chaubey and Malhotra 2002; Kausaite-Minkstimiene et al. 2014). All three electrodes were immersed in 10 mL of sterile PBS buffer. After applying the electrical potential the cell was allowed to stabilise electrochemically until the change in the electrical current was smaller than 100 pA/s. The amperometric measurements were performed under stirring at 350 rpm at which the noise associated with the magnetic stirrer was less than 5 nA.

2.5 Microneedle CGM Device

The microneedle CGM device consisted of working, counter and reference electrodes. All three microneedle electrodes were fabricated using a master mould consisting of 32 needles of about 1.5 mm in length. Details on the microneedles length requirements are provided in Supporting Information, section 4. The SU8 photoresist polymer was used to produce the microneedle arrays. The sensing layer at the working electrode was fabricated using the same method as the SM sensors with the addition of PU. 1.33 mL PU (2.67mg/mL in THF) was spray coated onto the three electrodes as the last deposition step to preserve the integrity of the sensing layer during in-vivo testing. The counter electrodes were spray coated with the same graphene ink applied at the working electrode as the conductive layer. The reference electrodes were produced by spray coating 1 mL Ag/AgCl ink ($1g/1mL_{MEK}$) followed by curing at 65°C for 1 hour and one week curing at room temperature. The three electrodes were then lowered in melted paraffin wax at 75°C which provided electrical isolation for the backplane of the microneedles. This would minimise noise during in-vivo testing due to perspiration.

3 Results & Discussion

3.1 Sensing Layer Characterisation

The uniformity of TTF throughout the sensing layer was investigated using SEM and EDX techniques. Studies were performed to determine the distribution of the sensing elements, i.e. TTF and GOx, at the surface of the electrodes (planar surface) and through the sensing layer (cross section).

3.1.1 Planar Surface Analysis

The SEM images and EDX elemental mapping at the planar surface of DL, SL and SM sensors are shown in Figure 1. Carbon, GOx, TTF, and GA were deposited onto silicon substrates using the DL, SL and SM techniques. The presence of TTF in the sensing layer was indicated by the sulphur EDX map as shown in Figure 1. Sulphur distribution at the surface was studied, since uniform deposition of TTF is the main interest here. Figure 1 shows the SEM images and EDX mapping analysis for sulphur (i.e. associated with TTF) at the planar surface in typical DL, SL and SM samples. The EDX map for the DL samples exhibited much stronger sulphur signal intensity (highlighted by green circle in Figure 1) near the edges of a waxed window which indicated the presence of the ‘coffee-ring’ effect and

therefore non-uniformity of the TTF. In addition, the formation of the TTF crystals, especially around the edges of a silicon substrate, was observed using an optical microscope (see Supporting Information, Figure S4). The planar distribution of carbon and oxygen was also studied in DL samples and showed a corresponding decrease in carbon at the edges where the TTF had accumulated (see Supporting Information, Figure S5). In contrast to the DL samples, a uniform distribution of the TTF was observed for the SL and SM samples as shown in Figure 1. AFM studies also confirmed the formation of large crystals at the surface of DL sample whereas a much smoother surface was observed in SL and SM samples as shown in Figure S6.

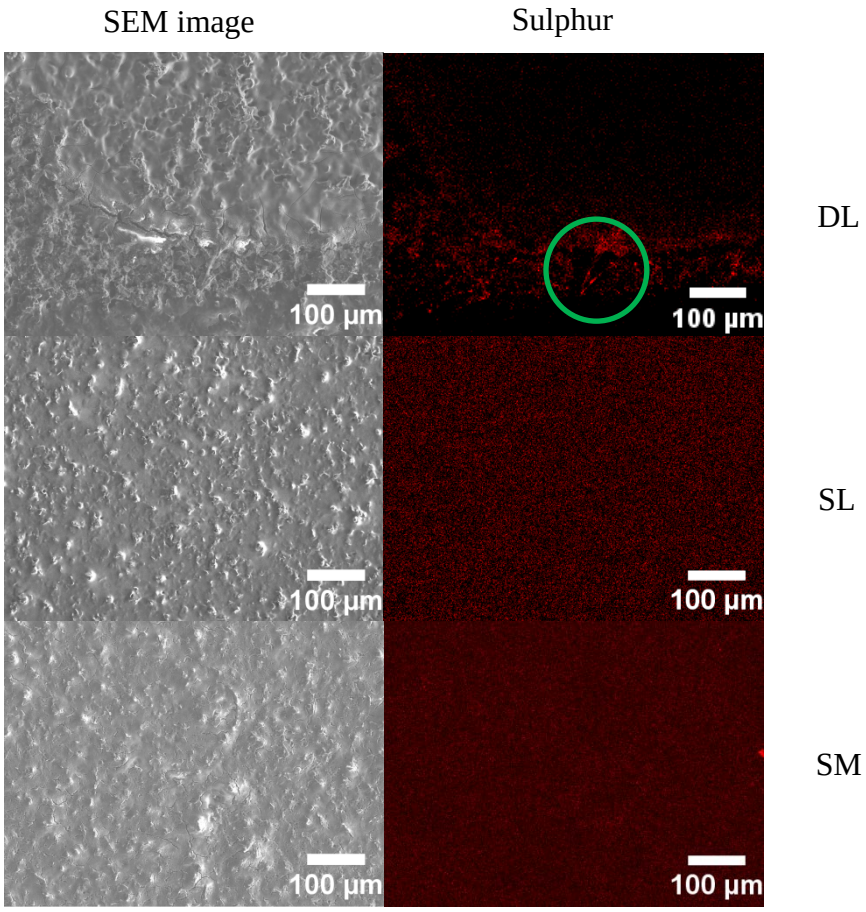

Figure 1: SEM images (left) and EDX map of the sulphur (right) at the planar surface for the DL, SL and SM fabricated sensors.

3.1.2 Cross-sectional Analysis

For the cross-sectional SEM and EDX studies, separate samples were fabricated with 10 fold increase in the deposited TTF as compared to the planar surface samples in order to enhance

the EDX sulphur signal originating from TTF in both SM and SL samples to a detectable range, thus allowing the study of uniformity throughout the sensing layer. This had led to a TTF layer which could be observed clearly in the SEM images (see Supporting Information, Figure S7). The biological components, GOx and GA were indicated by carbon and oxygen peaks in the EDX (note that the conductive carbon layer was not deposited onto the substrate for the cross-sectional studies to avoid confusion on the carbon peak especially in the SM case). TTF also contains carbon in its molecular structure; however the EDX results on the SL sample in Figure 2(a) shows negligible carbon peak in the pure TTF region on the right hand side of the image. Also, there was a good correlation between the carbon and oxygen levels in the outer layer as observed in Figure 2(a) which confirmed the carbon peak was dominated by the presence of GOx and GA rather than TTF. The Si peak was due to the underlying silicon substrate in all EDX results. The cross-sectional EDX analysis allowed the study of the mixing of the biological components and the mediator throughout the sensing layer for the SL sample in comparison to the SM sample. The DL sample was not discussed here due to the formation and non-uniform distribution of large TTF crystals across the surface as reported in previous section. For the SL sample, Figure 2(a) shows a strong EDX signal for carbon and oxygen (associated with the GOx and GA) at the top of the sensing layer (i.e. left hand side of the image). As the line profile reached the TTF layer, the EDX signal for carbon and oxygen dropped almost to zero while the signal for sulphur reached maximum. This showed the layer-by-layer formation with GOx and GA compounds as the top layer and TTF as the bottom layer for the SL sample which indicated a limited contact area between the GOx and TTF. The SM sample, on the contrary, showed a uniform distribution of sulphur (representing TTF), carbon and oxygen (both representing the biological components) from top to bottom of the sensing layer (i.e. left to right in Figure 2(b)). For both SL and SM samples as the line profile reaches the silicon substrate on the right hand side of the images in Figure 2, the EDX signal for carbon, oxygen, and sulphur decreases and silicon increases.

The uniform mixing of the TTF mediator and the biological components (i.e. GOx and GA), which are typically immiscible (Nielsen et al. 2000; Singer 1963; Zaks and Klibanov 1985), throughout the sensing layer makes the SM deposition technique ideal for applications where the integration of two immiscible compounds is important.

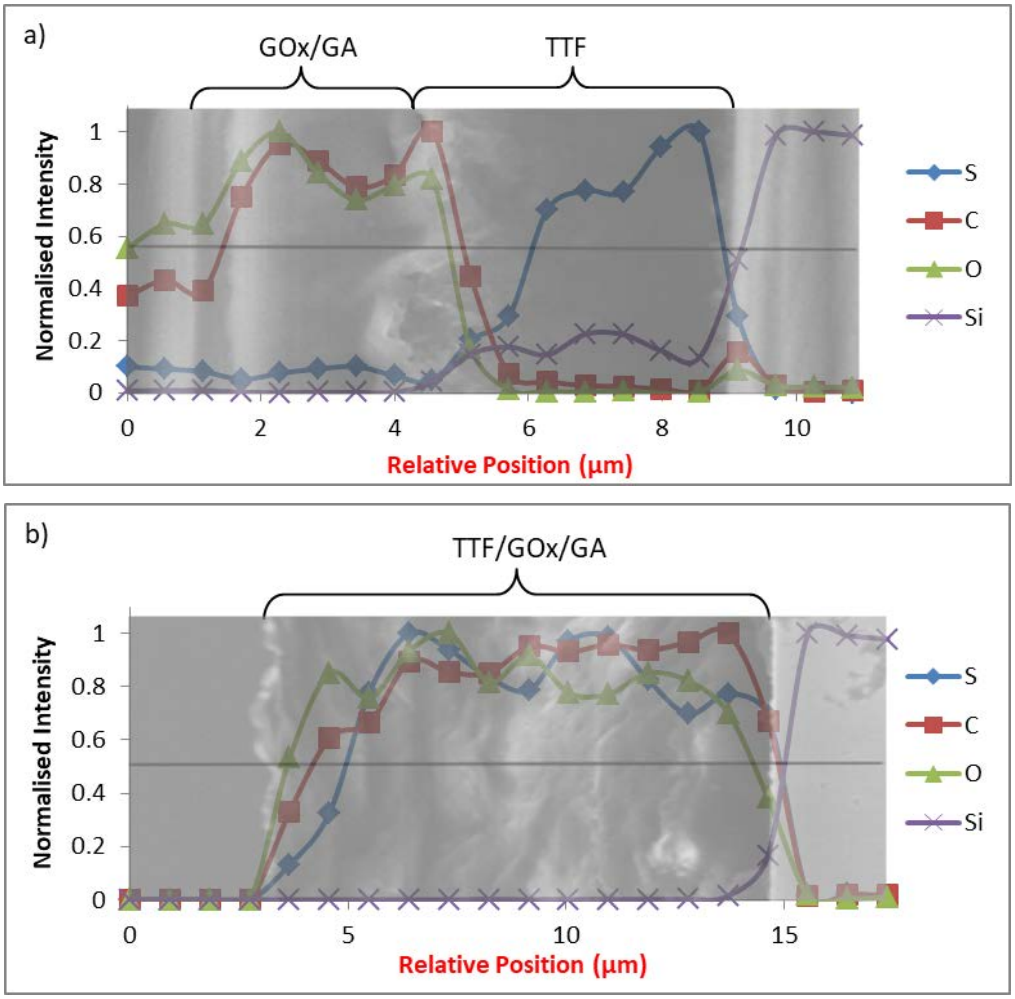

Figure 2: Cross-sectional EDX analysis for a) SL and b) SM techniques. The EDX signal for each element was normalised by its maximum number of counts.

3.2 Amperometric Sensor Performance

The amperometric response of DL, SL and SM glucose sensors shown in Figure 3 was studied against successive additions of glucose until the current response reached a plateau at saturation point showing the characteristics of the Michaelis-Menten kinetics (Salimi et al. 2007). Figure 3(a), (b) and (c) illustrate the amperometric response of the DL, SL, and SM glucose sensors with 5 repeats respectively. Figure 3(d) shows the average I_{max} parameter representing maximum limit of the amperometric current response and the maximum enzymatic reaction rate at saturation point (Kano and Ikeda 2000).

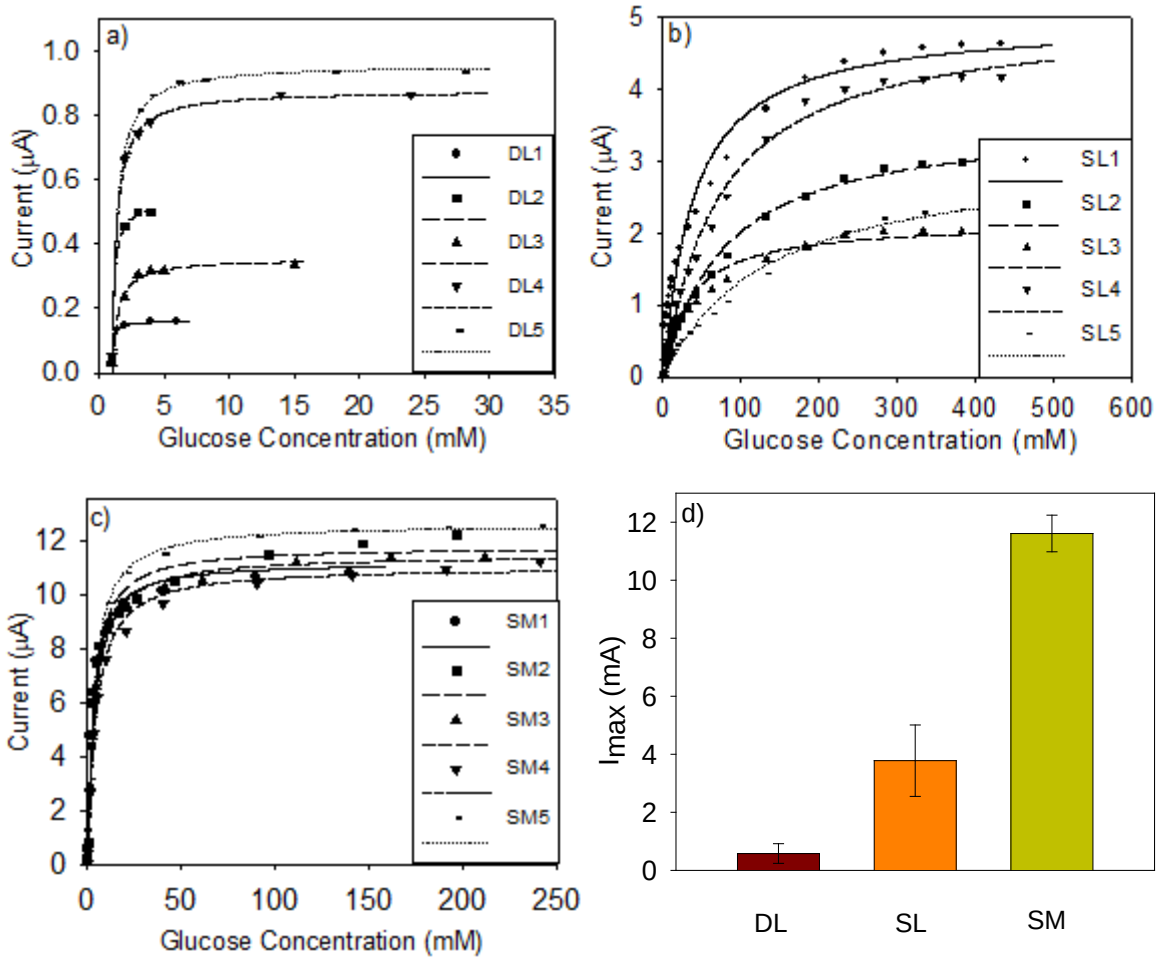

Figure 3: The amperometric response to glucose additions for the a) DL, b) SL and c) SM sensors and d) the average I_{max} values for DL, SL, and SM sensors. The legends represent measurements taken from 5 sensors fabricated using the same method (n=5).

The DL sensors exhibited the smallest amperometric response to glucose additions compared to both SL and SM sensors. The poor performance of the DL sensors shown in Figure 3(a) and (d) could be associated with the random formation of large TTF crystals at the surface of the electrode (see Figures S4, S5 and S6), which would significantly decrease the active interface between TTF and GOx, hence restricting the redox reaction between the two materials. The SL sensors in Figure 3(b) showed a larger average I_{max} than the DL sensors. The increase in the performance of the SL sensors could indicate the enhanced redox reaction as a result of better proximity between the mediator and enzyme due to TTF and GOx aerosols landing uniformly onto the surface forming smaller and more uniformly distributed TTF crystals across the surface hence enhancing the TTF-GOx reaction surface area (see Figure S5).

The SM sensors in Figure 3(c) and (d) show a much larger average I_{max} than both the DL and SL sensors. Two phenomena could account for the observed increase in the I_{max} for the SM sensors. Firstly, the closer proximity between the immobilised TTF and GOx as a result of better mixing enhances the redox reaction and the amperometric signal (Chaubey and Malhotra 2002; Chen et al. 2013). Secondly, the improved electron transfer via the TTF throughout the sensing layer would significantly increase the current signal (Chen et al. 2013; Trzebinski et al. 2012). As discussed previously the SEM and EDX analysis showed an enhanced uniformity in TTF and GOx distribution across and throughout the sensing layer of SM sensors. This is in good agreement with the observed significantly better I_{max} in the SM sensors as shown in Figure 3 due to an improved enzyme-mediator interface as a result of uniform distribution of TTF throughout the sensing layer.

The average sensitivity of the SM glucose sensors was derived from the amperometric studies (in Figure 3) over a linear range of 2 to 6 mM and was found to be an order of magnitude larger than both the SL and DL sensors which was in good agreement with the I_{max} analysis (see Figure S8). This study showed a significant improvement in the sensitivity due to spray mixing of the mediator and enzyme as aerosols, which cannot be achieved by conventional deposition methods such as drop casting the compounds (Kausaite-Minkstimiene et al. 2014).

It has been reported that PU was used in glucose sensors as a biocompatible polymer to enhance the linear range of glucose sensors, to reduce interference and to protect the sensing layer which is suitable for implantable devices (Jaffari and Pickup 1996; Ribet et al. 2017; Trzebinski et al. 2012; Vasylieva et al. 2015). In this study, the spray coated PU on the sensing layer led to an increase in linear range up to 20 mM (see Figure S9). The selectivity of best performing glucose sensors (i.e. SM sensors) was initially studied via cyclic voltammetry (CV) where 0.2 mM of uric acid (UA) and ascorbic acid (AA) was added during the CV measurements followed by 5 mM of glucose addition after the CV signal was settled as shown in Figure 4(a). These concentrations were chosen according to the physiological concentrations in human body as reported previously (Zhong et al. 2017). The CV oxidation signal in Figure 4(a) showed a significantly smaller response to uric acid and ascorbic acid at working potentials of about 0.22 V and hence was applied to the subsequent chronoamperometric studies. The typical current response for interfering compounds and glucose is shown in Figure 4(b). Current response for the interfering electroactive species were normalized to that of glucose as shown in Figure 4(c). The normalised current response

to ascorbic acid was about 20% and larger than uric acid interference, which was consistent with previously reported work (Amor-Gutiérrez et al. 2017; Rong et al. 2007; Zhao et al. 2018).

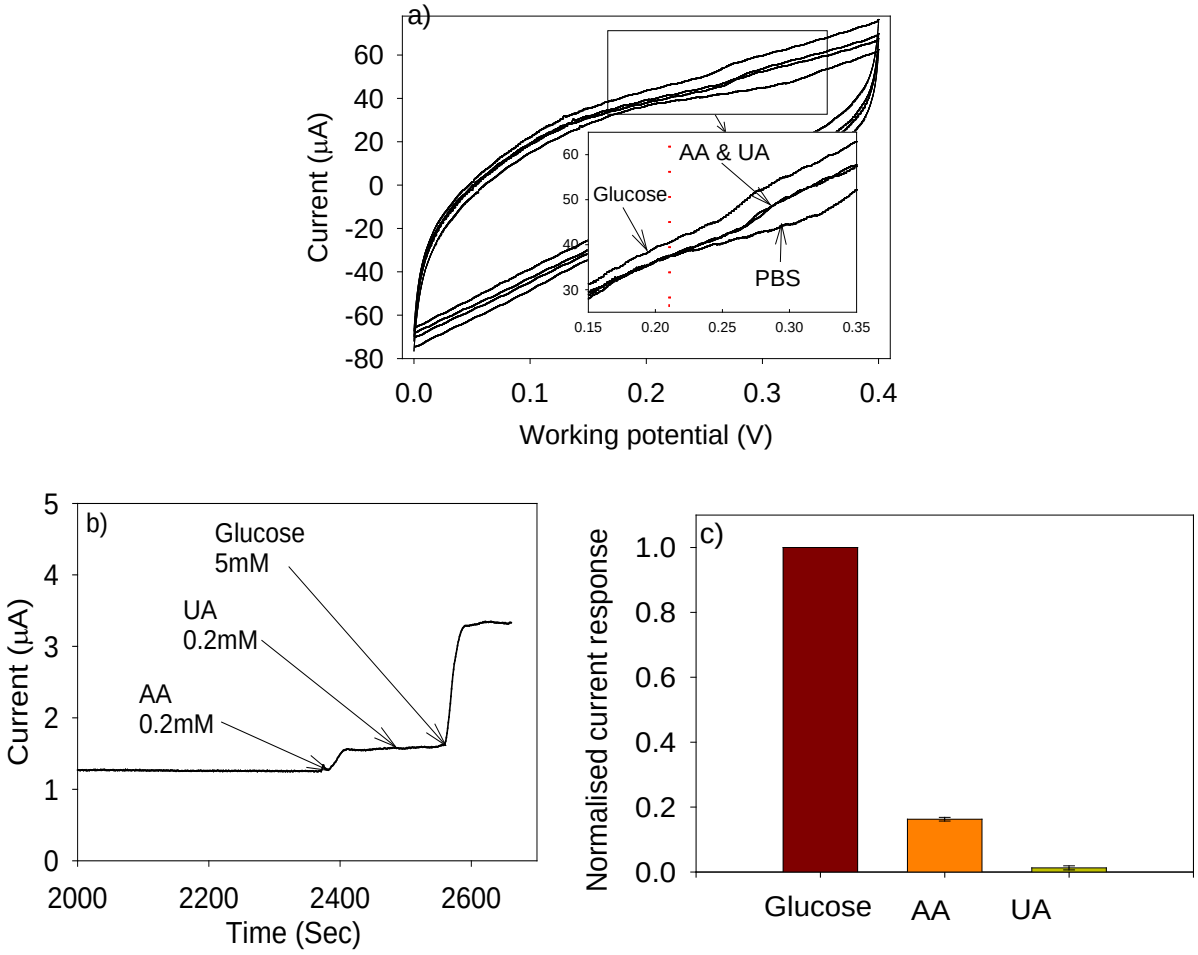

Figure 4: (a) Typical selectivity via cyclic voltammetry; inset shows the zoomed in CV current change due to addition of 0.2 mM AA, 0.2 mM UA, and 5 mM glucose each after 6 cycles. The red dashed line indicates the 0.22 V working potential. CV measurements were performed at 100 mV/sec. (b) typical selectivity via amperometric response at 0.22 V working potential, and (c) the average amperometric response to AA and UA normalised by the current response to glucose at 0.22 V, n=3.

3.2.1 Microneedle CGM Device

Microneedle CGM device only disrupts the outer skin layer (e.g. epidermis) to access interstitial fluids (ISF) with negligible pain (Donnelly et al. 2010; Kim et al. 2012; Prausnitz 2004) as opposed to current commercially available CGM devices requiring much deeper skin penetration with great discomfort. This has led to recent development of minimally

invasive microneedle devices for diagnostics (Esfandyarpour et al. 2013; Miller et al. 2016; Mohan et al. 2017; Valdés-Ramírez et al. 2014) . The SM technique developed in this work was ideal in producing uniformly coated and mixed sensing layer onto 3D structures, such as the microneedle electrodes of the minimally invasive CGM devices.

The integrity of the sensing layer was investigated by inserting the microneedle sensors into pork skin prior to in-vivo testing. The SEM images in Figure 5(a) and (b) show no sign of damage to the sensing layer after the insertion. In-vivo assessment of the microneedles was carried out on fasting healthy individuals (Details on the CGM in-vivo test are provided in Supporting Information, section 9). The amperometric current response from the microneedle CGM device was then monitored and compared to the finger prick blood glucose measurements performed every 15 min shown as red dots in Figure 5(c). In total, three in-vivo tests were performed on healthy individuals using three fabricated CGM devices. A typical CGM measurement is shown in Figure 5(c) and the other two repeats can be found in Figures S11 and S12 in the Supporting Information. An average lag time of 20 min was observed in the in-vivo amperometric response as compared to the finger prick data in response to glucose. This lag time was due to two diffusional components, firstly the time taken for glucose to diffuse from blood vessels to the ISF which is about 8-10 mins on average (Cengiz and Tamborlane 2009; Roe and Smoller 1998), and secondly the diffusional limitation in the epidermis prohibiting ISF movement through to the sensing layer. After compensating for this lag time as shown in Figure 5(c) the finger prick data overlapped quite consistently with the amperometric response showing good agreement between the microneedle CGM device and the standard finger prick readings. The observed amperometric response in the in-vivo test was roughly three orders of magnitude smaller than that from the beaker test. This could be due to the much smaller surface area of the needles in touch with the basal layer of the epidermis which possess the largest amount of ISF. For this reason, it is of paramount importance that the sensitivity of the microneedle glucose sensor was enhanced through the SM deposition technique.

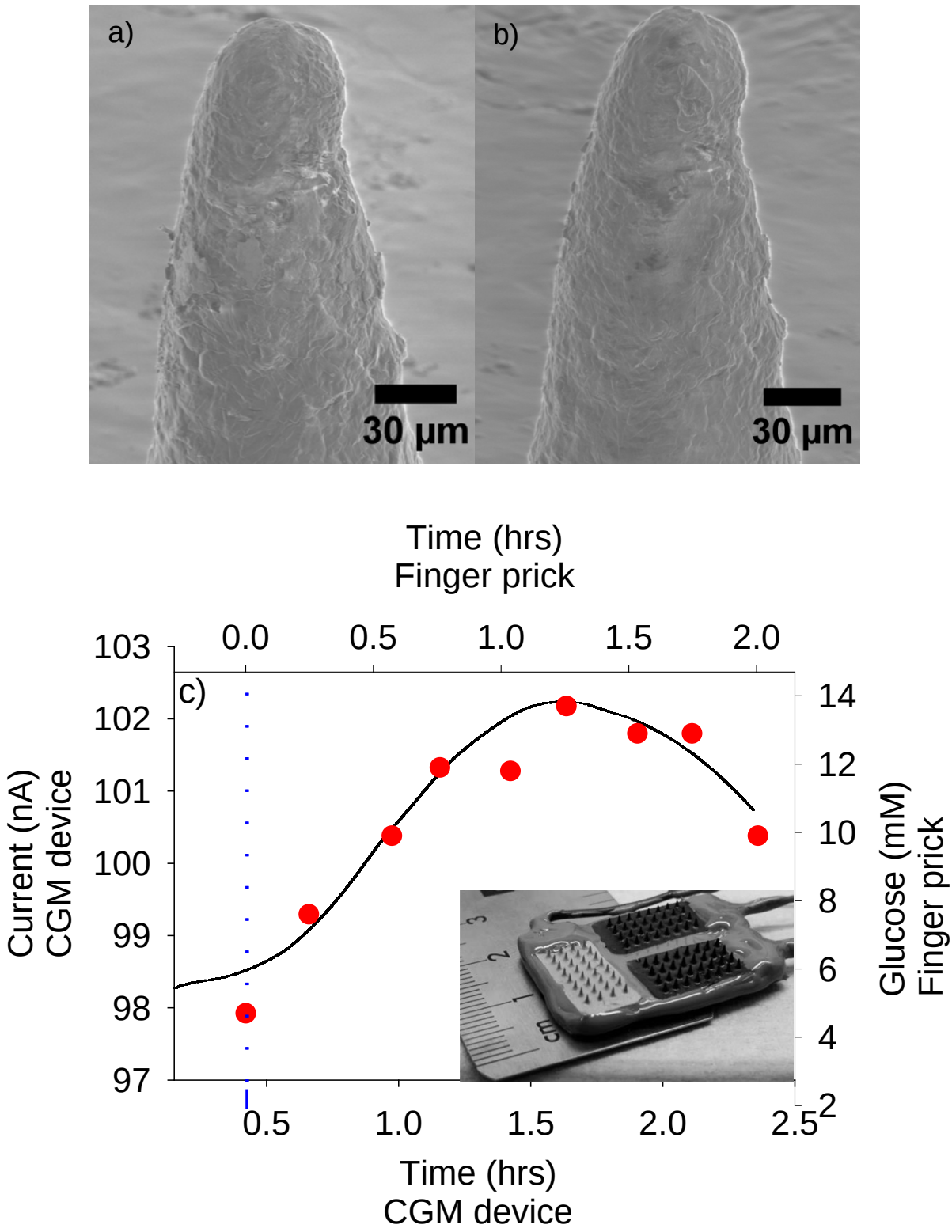

Figure 5: The SEM images of a typical working electrode needle (a) before and (b) after insertion into pig skin. (c) The amperometric data from the in-vivo microneedle CGM device overlapped with the finger prick readings; (inset) optical image of the CGM device. The blue dashed line indicates the time at which Polycal was consumed by the volunteer.

4 Conclusion

This work demonstrated the novel application of spray coating as a simple, low-cost and mass producible fabrication technique to produce a uniformly mixed sensing layer from immiscible compounds such as GOx and TTF. SEM and EDX studies on the SM samples showed that the two compounds were distributed evenly throughout the sensing layer in both planar and cross-sectional studies. The amperometric measurement studies confirmed a direct correlation between the uniform mixing of the GOx/TTF compounds and maximum current response, I_{max}. The uniform mixing of the compounds led to an order of magnitude larger sensitivity of the SM sensors as compared to both the DL and SL sensors. In addition good selectivity was achieved against ascorbic acid and uric acid. Using the SM technique, a minimally invasive microneedle CGM device was developed. The in-vivo amperometric studies of the CGM device were in good agreement with variations in blood glucose measured using the finger prick technique. The novel use of the SM technique in depositing immiscible sensing compounds uniformly onto 3D microneedle arrays can lead to the mass production of minimally invasive CGM devices at very low-cost with excellent performances.

Acknowledgement

The authors acknowledge the funding from the Welsh Government via the Life Science Bridging Fund Awards (i.e. LSBF/R1-007 and LSBF/R6-004-FoF). The authors would also like to acknowledge Sarah Dowrick and the Joint Clinical Research Facility in Swansea University for their help and support with regards to the clinical aspects.

Ethical Approval

Ethical approval was given by Swansea University Medical School Research Ethics Sub Committee (Ref: 2017-0031) and consent approval was sought from each volunteer prior to in-vivo assessment of the microneedle CGM device.

References

Amor-Gutiérrez, O., Costa Rama, E., Costa-García, A., Fernández-Abedul, M.T., 2017. Paper-based maskless enzymatic sensor for glucose determination combining ink and wire electrodes. Biosensors and Bioelectronics 93, 40-45.

Chaubey, A., Malhotra, B.D., 2002. Mediated biosensors. Biosensors and Bioelectronics 17, 441.

Chen, C., Xie, Q., Yang, D., Xiao, H., Fu, Y., Tan, Y., Yao, S., 2013. Recent advances in electrochemical glucose biosensors: a review. RSC Advances 3(14), 4473-4491.

Donnelly, R.F., Singh, T.R.R., Woolfson, A.D., 2010. Microneedle-based drug delivery systems: Microfabrication, drug delivery, and safety. Drug Delivery 17(4), 187-207.

Esfandyarpour, R., Esfandyarpour, H., Javanmard, M., Harris, J.S., Davis, R.W., 2013. Microneedle biosensor: A method for direct label-free real time protein detection. Sensors and Actuators B: Chemical 177, 848-855.

Haiying, L., Jiaqi, D., 1995. Amperometric glucose sensor using tetrathiafulvalene in Nafion gel as electron shuttle. Analytica Chimica Acta 300(1), 65-70.

Hale, P.D., Inagaki, T., Karan, H.I., Okamoto, Y., Skotheim, T.A., 1989. A new class of amperometric biosensor incorporating a polymeric electron-transfer mediator. Journal of the American Chemical Society 111(9), 3482-3484.

Jaffari, S.A., Pickup, J.C., 1996. Novel hexacyanoferrate (III)-modified carbon electrodes: application in miniaturized biosensors with potential for in vivo glucose sensing. Biosensors and Bioelectronics 11(11), 1167-1175.

Kano, K., Ikeda, T., 2000. Fundamentals and practices of mediated bioelectrocatalysis. Analytical Sciences 16, 1013.

Kausaite-Minkstimiene, A., Mazeiko, V., Ramanaviciene, A., Oztekin, Y., Solak, A.O., Ramanavicius, A., 2014. Evaluation of Some Redox Mediators in the Design of Reagentless Amperometric Glucose Biosensor. Electroanalysis 26, 1528.

Kim, Y.-C., Park, J.-H., Prausnitz, M.R., 2012. Microneedles for drug and vaccine delivery. Advanced Drug Delivery Reviews 64(14), 1547-1568.

Liu, C.-H., Yu, X., 2011. Silver nanowire-based transparent, flexible, and conductive thin film. Nanoscale Research Letters 6, 75.

Mathers, C.D., Loncar, D., 2006. Projections of Global Mortality and Burden of Disease from 2002 to 2030. PLOS Medicine 3, 442.

Miller, P.R., Narayan, R.J., Polsky, R., 2016. Microneedle-based sensors for medical diagnosis. Journal of Materials Chemistry B 4(8), 1379-1383.

Mohan, A.M.V., Windmiller, J.R., Mishra, R.K., Wang, J., 2017. Continuous minimally-invasive alcohol monitoring using microneedle sensor arrays. Biosensors and Bioelectronics 91, 574-579.

Nielsen, M.B., Lomholt, C., Becher, J., 2000. Tetrathiafulvalenes as building blocks in supramolecular chemistry II. Chemical Society Reviews 29, 153-164.

Prausnitz, M.R., 2004. Microneedles for transdermal drug delivery. Advanced Drug Delivery Reviews 56(5), 581-587.

Ribet, F., Stemme, G., Roxhed, N., 2017. Ultra-miniaturization of a planar amperometric sensor targeting continuous intradermal glucose monitoring. Biosensors and Bioelectronics 90, 577 - 583.

Rong, L.-Q., Yang, C., Qian, Q.-Y., Xia, X.-H., 2007. Study of the nonenzymatic glucose sensor based on highly dispersed Pt nanoparticles supported on carbon nanotubes. Talanta 72(2), 819-824.

Salimi, A., Sharifi, E., Noorbakhsh, A., Soltanian, S., 2007. Immobilization of glucose oxidase on electrodeposited nickel oxide nanoparticles: Direct electron transfer and electrocatalytic activity. Biosensors and Bioelectronics 22(3146-3153).

Singer, S.J., 1963. The Properties of Proteins in Nonaqueous Solvents. Adv. Protein Chem. 17, 1-68.

Trzebinski, J., Sharma, S., Moniz, A.R.B., Michelakis, K., Zhang, Y., Cass, A.E.G., 2012. Microfluidic device to investigate factors affecting performance in biosensors designed for transdermal applications. Lab on a Chip 12, 348.

Valdés-Ramírez, G., Li, Y.-C., Kim, J., Jia, W., Bandodkar, A.J., Nuñez-Flores, R., Miller, P.R., Wu, S.-Y., Narayan, R., Windmiller, J.R., Polsky, R., Wang, J., 2014. Microneedle-based self-powered glucose sensor. Electrochemistry Communications 47, 58-62.

Vasylieva, N., Marinesco, S., Barbier, D., Saba, A., 2015. Silicon/SU8 multi-electrode micro-needle for in vivo neurochemical monitoring. Biosensors and Bioelectronics 72, 148-155.

Wilson, R., Turner, A.P.F., 1992. Glucose-oxidase-An ideal enzyme. Biosensors and Bioelectronics 7, 165-185.

Zaks, A., Klibanov, A.M., 1985. Enzyme-catalyzed processes in organic solvents. Proc. Natl. Acad. Sci. USA 82, 3192-3196.

Zhao, W., Zhang, R., Xu, S., Cai, J., Zhu, X., Zhu, Y., Wei, W., Liu, X., Luo, J., 2018. Molecularly imprinted polymeric nanoparticles decorated with Au NPs for highly sensitive and selective glucose detection. Biosensors and Bioelectronics 100, 497-503.

Zhong, S.L., Zhuang, J., Yang, D.P., Tang, D., 2017. Eggshell membrane-templated synthesis of 3D hierarchical porous Au networks for electrochemical nonenzymatic glucose sensor. Biosensors and Bioelectronics 96, 26-32.

Graphical Abstract